24. Brownlee, D. E. *Ann. Rev. Earth planet. Sci.* **13,** 147–173 (1985).
25. Amari, S. & Ozima, M. *Geochim. cosmochim. Acta* **52,** 1087–1095 (1988).
26. Fukumoto, H., Nagao, K. & Matsuda, J. I. *Geochim. cosmochim. Acta* **50,** 2245–2253 (1986).
27. Nier, A. O. & Schlutter, D. J. *Meteoritics* **25,** 263–267 (1990).
28. Schultz, L. & Kruse, H. *Meteoritics* **24,** 155–172 (1989).
29. Maurette, M., Hammer, D. & Pourchet, M. in *From Mantle to Meteorites* (eds Gopalan, K., Gaur, V. K., Somayajuju, B. L. & MacDougall, J. D.) (Indian Academy of Sciences, Bangalore, 1990).

SUPPLEMENTARY INFORMATION. Requests should be addressed to the London editorial office of *Nature*.

ACKNOWLEDGEMENTS. We thank R. M. Walker, D. Brownlee and C. M. Hohenberg for helpful discussions, and P. Galle and P. Siry for help. Funding for the Cap Prudhomme expedition was granted by 'Expéditions Polaires Francaises' and 'Terres Australes et Antarctiques Francaises'. Financial support is acknowledged from IN2P3 and INSU in France, 'Fonds zur Förderung der wissenschaftlichen Forschung' in Austria, and NASA.

Structural origin of reduced critical currents at $YBa_2Cu_3O_{7-\delta}$ grain boundaries

M. F. Chisholm & S. J. Pennycook

Solid State Division, Oak Ridge National Laboratory, Oak Ridge, Tennessee 37831-6024, USA

THE critical current density across individual grain boundaries in thin films of the high-T_c superconductor $YBa_2Cu_3O_{7-\delta}$ (YBCO) has been found[1–4] to be inversely proportional to lattice misorientation for tilts up to ~10°. Reports of impurity segregation[5,6] at grain boundaries, and variations in the chemical stoichiometry[7,8], have led to the view that deviations from the ideal composition are responsible for the depressed superconducting order parameter at the boundary. Here we present images of YBCO grain boundaries obtained by a scanning transmission electron microscope in Z-contrast mode[9,10], which show that chemical segregation does not necessarily occur at these boundaries. A simple model of the strain associated with the grain-boundary dislocations provides a reasonable physical explanation of the suppressed superconductivity. The surprisingly large effect of strain implied by our model has implications beyond critical currents, for the physics and applications of any thin-film YBCO structures involving strained epitaxial layers.

In epitaxial thin films of $YBa_2Cu_3O_{7-\delta}$ on polycrystalline $SrTiO_3$, the critical current density across a grain boundary decreases drastically with increasing misorientation angle,[1–4] and the boundary behaves as a weak link for misorientations greater than 10°. Recent results from bulk-scale bicrystals, however, have indicated that certain high-angle grain boundaries do not exhibit this weak-link response[11]. No satisfactory microscopic explanation for the origin of this behaviour of grain boundaries has so far been proposed[3,12]. Additionally, it has structural models of low-angle boundaries do not lead to the observed angular dependence of the transport critical current[2,4,12]. The most commonly accepted view is that deviations from the ideal stoichiometry are responsible for the low critical current densities[13]. There are several reports of compositional variations at grain boundaries[5–8], but only small decreases in already low critical current densities have been directly correlated with deviations from the stoichiometric composition in the boundary regions[8].

We have used the Z-contrast technique[9,10] for forming chemically sensitive high-resolution images in a scanning transmission electron microscope (VG Microscopes HB501UX STEM operating at 100 kV) to investigate the composition of YBCO grain boundaries. In this technique, a fine electron beam of width 0.22 nm (full width at half maximum intensity) is scanned across the sample, and the electrons scattered at high angles are collected by an annular detector and used to form an image. The high-angle scattering is proportional to Z^2, where Z is the atomic number of the species under the probe. Thus the image can be thought of as a map showing at atomic resolution the scattering power of the sample[9,10]. This technique can provide analysis of regions of the sample down to a size comparable to the superconducting coherence length. We have examined boundaries of the same type as those investigated in refs 1–4. Such tilt boundaries consist of an array of uniformly spaced edge dislocations produced to accommodate the mismatch[14]. Our grain-boundary samples were taken from polycrystalline thin films of $YBa_2Cu_3O_{7-\delta}$ grown on Y_2O_3-stabilized ZrO_2 and from a pellet of sintered powder. Figure 1 shows Z-contrast images of a 13° tilt boundary at which the adjacent grains nearly share a common [100] direction. In Fig. 1*a* the beam passes parallel to the crystal planes of both grains, which are seen to be separated by an array of triangular defects. The planes of barium atoms ($Z = 56$) show higher intensity than the yttrium ($Z = 39$) planes, and terminate both grains along the long sides of the triangular zones. Phase-contrast imaging using the STEM bright-field detector clearly shows that these faceted dislocation cores are amorphous. To determine whether the amorphous material has the same composition as the crystalline superconductor, it is necessary to tilt the right-hand grain by a few degrees so that the clear image of the crystal planes is lost. The intensity scattered by the crystal in a random orientation will equal the intensity scattered by a random (amorphous) arrangement having the same overall composition. The contrast in the annular detector signal can be quantified very simply using appropriate screened cross-sections for elastic scattering[15]. Thus we can probe any segregation to the amorphous zones with a sensitivity limited by the image statistics and by the extent to which we can avoid thickness variations and residual channelling effects, which we estimate to be ±2%.

Within this limit no contrast changes are detectable between the amorphous zones and the randomly oriented crystal (Fig. 1*b*). Similar results were obtained from other tilt boundaries, including a 34° high-angle (high-energy) tilt boundary. This rules out the presence of any of the likely phases, including $Y_2Ba_4Cu_7O_{14}$, $YBa_2Cu_4O_8$ and $BaCuO_2$, and sets limits to the range of stoichiometry that would not be detectable as

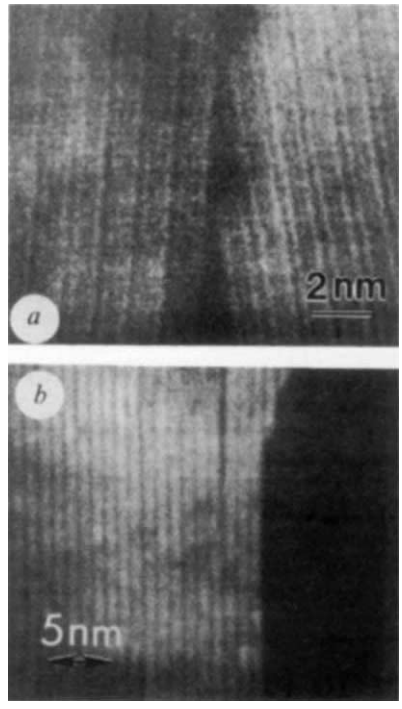

FIG. 1 Z-contrast images of a 13° [100] tilt boundary. *a*, Both grains oriented for electron channelling along the (001) planes, showing an array of triangular amorphous zones at the boundary. *b*, Sample tilted so that the right-hand grain is not channelling, showing no detectable contrast variations along the grain boundary.

$Y_{0.87\leq x\leq 1.13}Ba_{1.92\leq x\leq 2.07}Cu_{2.79\leq x\leq 3.21}O_{4.91\leq x\leq 9.09}$, where only one component is assumed to vary at a time. The method is rather insensitive to oxygen because of its relatively low atomic number, but given the high mobility of oxygen at low temperatures[16] it seems doubtful that any microscopic measurement on a thin specimen could provide meaningful oxygen contents. We estimate the spatial resolution of our measurement to be 1 nm, significantly better than has been achieved using X-ray fluorescence. This resolution is possible because the number of elastically scattered electrons detected is typically 10^5 times greater than the number of X-rays collected from the same area, allowing us to work with thicknesses of only 10–20 nm, which greatly reduces beam-broadening effects. Our results therefore represent the most sensitive measurements so far of grain-boundary composition. They indicate clearly that, although compositional variations undoubtedly can occur, they are not necessarily present.

In the light of these results, we therefore re-examine structural models of grain boundaries and attempt to understand how a dislocation array can cause a large reduction in critical current. We start with the simplest model and assume that the order parameter for superconductivity is depressed only within a strained region associated with the grain-boundary dislocations, which we assume has a well defined radius, r_m, in the plane of the boundary. Therefore, the ratio of the critical current density across a grain boundary, J_c^{gb}, to that within the grain, J_c^G, is $(D-2r_m)/D$, where $D=|\mathbf{b}|/\sin\theta$ is the dislocation spacing, $\mathbf{b}$ is the Burgers vector of the dislocation, and θ is the tilt angle of the two adjacent grains. For small tilt angles,

$$J_c^{gb}/J_c^G = 1-\frac{2r_m}{|\mathbf{b}|}\theta \qquad (1)$$

That is, the normalized grain-boundary critical current density decreases linearly with θ for small misorientations. In Fig. 2 we show a linear plot of the data of Dimos *et al.*[4], which clearly shows this predicted linear behaviour in the small-angle regime. From a least-squares fit of the slope between $\theta=0°$ and 10°, we determine $r_m\simeq 2.9|\mathbf{b}|$, which is much larger than the value assumed previously[2,6].

We believe that the physical origin for this surprisingly large effect of a grain-boundary dislocation is that the superconducting properties of $YBa_2Cu_3O_{7-\delta}$ are very sensitive to strain. Superconductivity is produced in this normally antiferromagnetic insulator by the addition of charge to the CuO_2 planes[17]. Disruption of the charge reservoir layers, for example by disordering the Cu–O chain layers, will affect superconductivity adversely. A strain of only 1% along the *a* or *b* axis is required to prevent the transformation from a tetragonal to an orthorhombic structure during processing, interfering with the order in the Cu–O chain layers and leading to significant volumes of non-superconducting material surrounding each dislocation core. Independent support for this 1% criterion comes from particle irradiation experiments in which oxygen is displaced with no overall change in oxygen stoichiometry[18,19]. Extrapolating the data to one oxygen displacement per unit cell, which would destroy the orthorhombicity, predicts T_c to be depressed by ~100 K. Further indications of the importance of strain comes from observations on $Nd_{1.83}Ce_{0.17}CuO_x/YBa_2Cu_3O_{7-\delta}$ multilayers, in which 1% strains significantly affected the normal-state resistivity and the superconducting transition[20]. We therefore adopt 1% strain as the criterion for defining r_m, and calculate the strain field around an edge dislocation array parallel to the tilt axis assuming that linear isotropic elasticity theory is applicable[21]. Figure 3 is a plot of the roughly elliptical area around the dislocations in which one of the strain components is calculated to be ≥1%. Reduced distances are used so that the solutions for 2°, 5° and 10° tilt boundaries can be displayed. It can be seen that for all three cases there is a 'conducting plate' of relatively undistorted crystal between dislocations. For the 10° boundary, however, the thickness of this conducting plate is less than the dimensions of the unit cell, and thus the structural order required for superconductivity is destroyed everywhere along the boundary. For misorientation angles less than 10°, the equations for the extent of the 1% strain predict, to first order, linear dependence on misorientation angle, consisent with the available experimental data. The strong coupling observed by Mannhart *et al.*[3] in bicrystal films with less than 10° misorientation, where the magnetic-field dependence of the grain boundary critical current density was similar to that of a single crystal, is entirely consistent with our observation that for tilts of up to 10° there are regions of the boundary that are largely unaffected by the dislocations. The grain-boundary dislocations effectively only reduce the area of the grain-boundary plane. Therefore, our microscopic characterization of the structure and composition of the boundaries, and our calculations of the dislocation strain field provide a consistent and physical explanation of the critical current behaviour of individual boundaries.

Beyond 10° misorientations, the boundary loses the required structural order for superconductivity, provided that it cannot relax to a lower-strain configuration, and becomes a weak link which is very sensitive to small applied magnetic fields[3]. Bulk-scale bicrystal results[11] and observations of special high-angle misorientations where a coincidence site lattice is produced[23] indicate, however, that there are grain boundaries that can undergo further relaxations to reduce the boundary energy; some of these may not behave as weak links. Unfortunately, the strain field at the boundary cannot be predicted solely by using geometrical factors that describe the boundary periodicity, but depends also on their specific atomic structure. The observation

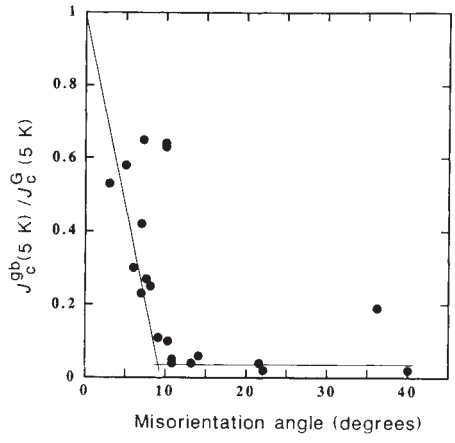

FIG. 2 Normalized critical current density as a function of misorientation[4], plotted on a linear scale.

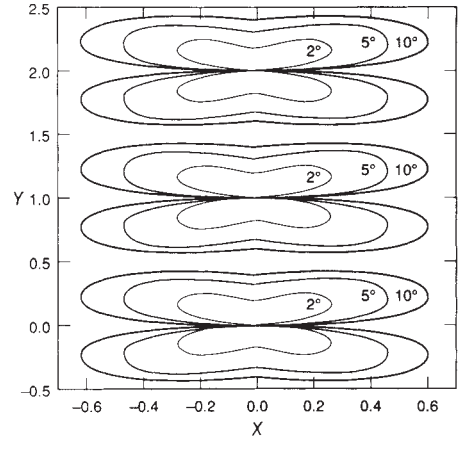

FIG. 3 Calculated strain field for an infinite array of edge dislocations at a 2°, 5° and 10° tilt boundary, showing the contour for a strain (ε_{xx}, the largest strain component) ≥1%, plotted using reduced distances $Y=y/D$ and $X=x/D$, where D is the dislocation spacing.

that a 14° boundary does not exhibit weak-link behaviour[11] does not necessarily contradict the strain model and, in fact, would seem to indicate that low-strain boundaries are not limited to high-coincidence orientations or, more probably, that the boundary contains segments of different structures, including a low-angle segment. The observation that 90° boundaries can sustain large critical currents[11,12] is entirely consistent with our model, because the dislocation array for such boundaries will be widely spaced. The structure of these and other special boundaries is currently under investigation. As it seems that the strain field, rather than the dislocations or boundaries themselves, is responsible for the suppression of superconductivity, the implications of our results are not limited to grain boundaries. The surprisingly large effect of strain will influence the superconducting properties of many artificial structures, such as superlattices and thin-film devices, which involve strains of the order of 1%. □

Received 27 December 1990; accepted 19 March 1991.

1. Chaudhari, P. *et al. Phys. Rev. Lett.* **60,** 1653-1656 (1988).
2. Dimos, D., Chaudhari, P., Mannhart, J. & LeGoues, F. K. *Phys. Rev. Lett.* **61,** 219-222 (1988).
3. Mannhart, J., Chaudhari, P., Dimos, D., Tsuei, C. C. & McGuire, T. R. *Phys. Rev. Lett.* **61,** 2476-2479 (1988).
4. Dimos, D., Chaudhari, P. & Mannhart, J. *Phys. Rev.* B **41,** 4038-4049 (1990).
5. Camps, R. A. *et al. Nature* **329,** 229-232 (1987).
6. Nakahara, S. *et al. J. Cryst. Growth* **85,** 639-651 (1987).
7. Babcock, S. E. & Larbalestier, D. C. *Appl. Phys. Lett.* **55,** 393-395 (1989).
8. Kroeger, D. M. *et al. J. appl. Phys.* **64,** 331-335 (1988).
9. Pennycook, S. J. & Boatner, L. A. *Nature* **336,** 565-567 (1988).
10. Pennycook, S. J. & Jesson, D. E. *Phys. Rev. Lett.* **64,** 938-941 (1990).
11. Babcock, S. E., Cai, X. Y., Kaiser, D. L. & Larbalestier, D. C. *Nature* **347,** 167-169 (1990).
12. Clarke, D. R., Shaw, T. M. & Dimos, D. *J. Am. Ceram. Soc.* **72,** 1103-1113 (1989).
13. Campbell, A. M. *Supercond. Sci. Technol.* **2,** 287-293 (1989).
14. Chisholm, M. F. & Smith, D. A. *Phil. Mag.* **A59,** 181-197 (1989).
15. Pennycook, S. J., Berger, S. D. & Culbertson, R J. *J. Microsc.* **144,** 229-249 (1986).
16. Rothman, S. J., Routbort, J. L. & Baker, J. E. *Phys. Rev.* B **40,** 8852-8860 (1989).
17. Cava, R. J. *Science* **247,** 656-662 (1990).
18. Summers, G. P., Burke, E. A., Chrisey, D. B., Natasi, M. & Tesmer, J. R. *Appl. Phys. Lett.* **55,** 1469-1471 (1989).
19. Marwick, A. D., Guarnieri, C. R. & Manoyan, J. M. *Appl. Phys. Lett.* **53,** 2713-2714 (1988).
20. Gupta, A. *et al. Phys. Rev. Lett.* **64,** 3191-3194 (1990).
21. Cottrell, A. H. *Dislocations and Plastic Flow in Crystals* (Clarendon Press, Oxford, 1953).
22. Chan, S.-W. *et al.* in *High T_c Superconducting Thin Films* Am. Inst. Phys. Conf. Proc. No. 200 (ed. Stockbour, R.) 172-189 (American Institute of Physics, New York, 1990).
23. Smith, D. A., Chisholm, M. F. & Clabes, J. *Appl. Phys. Lett.* **53,** 2344-2345 (1988).

ACKNOWLEDGEMENTS. This research was sponsored by the Division of Materials Sciences, US Department of Energy with Martin Marietta Energy Systems, Inc.

Surface-mediated alignment of nematic liquid crystals with polarized laser light

Wayne M. Gibbons, Paul J. Shannon, Shao-Tang Sun & Brian J. Swetlin

Research Center, Hercules Incorporated, Wilmington, Delaware 19894, USA

THE control of molecular alignment in liquid-crystal phases at macroscopic scales has been investigated extensively because of its importance in optical or optoelectronic applications, such as liquid-crystal displays[1]. It is well established that liquid crystals can be aligned by an applied electric field, a magnetic field, a shear-flow field, mechanical grooving of the substrate surface or stretching of liquid-crystal polymer thin films[2,3]. Here we report a new mechanism for liquid-crystal alignment that uses polarized laser light. We find that nematic liquid crystals in an illuminated region become oriented perpendicular to the direction of the electric-field polarization of the laser and remain aligned in the absence of the laser radiation. The liquid crystals can be reoriented again by subsequent illumination. This technique might have applications for large-area displays, optical memories, binary optics, adaptive optics and molecular micro-assembly.

We spin-coated a glass substrate with a thin layer of a silicone polyimide copolymer doped with a diazodiamine dye at a dye:polyimide weight ratio of 1:2. The chemical structure and absorption spectrum of the dye are shown in Fig. 1. We assembled a cell using this coated glass substrate as the top plate and a second glass substrate, coated only with polyimide, as the bottom plate, with a spacing of 11 μm between them. Both plates were rubbed with a cloth before assembly, the rubbing directions being matched on assembly. The cell was then filled with the nematic liquid crystal ZLI-1982 (EM Chemicals, Hawthorne, New York) at room temperature This is a eutectic mixture of phenylcyclohexane liquid crystal molecules. By using a polarization microscope, we observed the direction of the nematic phase to line up with the rubbing direction of the cell.

The cell was illuminated with a polarized argon ion laser (514.5 nm), with the direction of laser polarization parallel to the rubbing axis (Fig. 2). Within the illuminated region, the molecules of ZLI-1982 then assumed a twisted nematic structure. The molecules adjacent to the illuminated, dye-doped surface became oriented perpendicular both to their original direction and to the direction of the laser polarization, whereas molecules adjacent to the undoped polyimide surface remained aligned parallel to the rubbing direction. The image written in this way can therefore be seen with a pair of polarizers (Fig. 3). Similar control of liquid-crystal alignment was achieved by illuminating

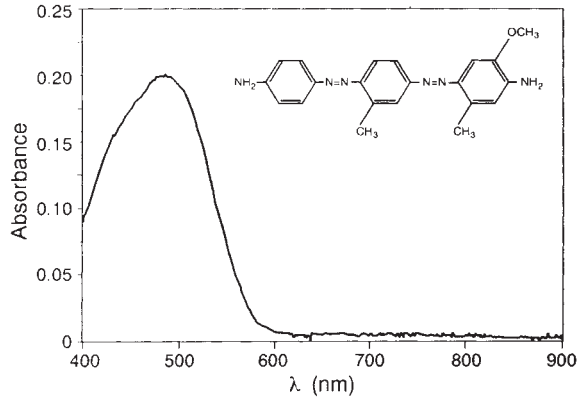

FIG. 1 The chemical structure and absorption spectrum of the dye dopant in the polyimide surface layer.

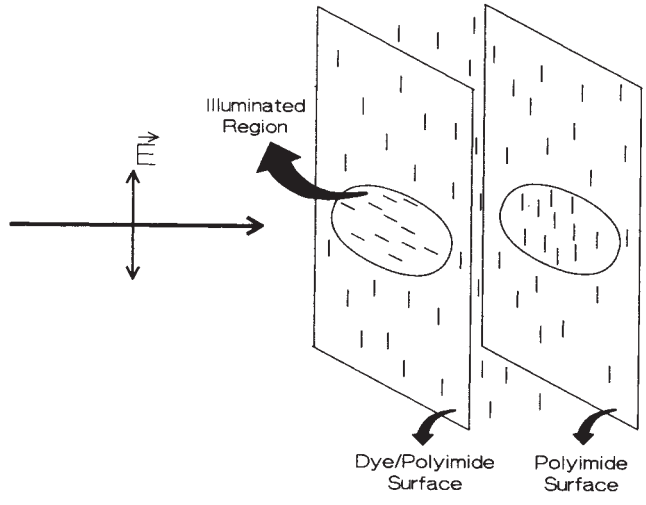

FIG. 2 The geometry of the illuminated liquid-crystal cell. The glass substrates of the cell are not shown for clarity. The rods represent the liquid-crystal orientation near the substrates before and after illumination.